coatings

MDPI

Article

Colorimetric Measurement of Deltamethrin Pesticide Using a Paper Sensor Based on Aggregation of Gold Nanoparticles

Jingyang Zhu [1], Lifeng Yin [1], Weiyi Zhang [2], Meilian Chen [2], Dongsheng Feng [2], Yong Zhao [1,*] and Yongheng Zhu [1,*]

[1] Laboratory of Quality & Safety Risk Assessment for Aquatic Products on Storage and Preservation (Shanghai), College of Food Science and Technology, Shanghai 201306, China; 15837688323@163.com (J.Z.); onlylihong666@163.com (L.Y.)
[2] Shanghai Center of Agri-Products Quality and Safety (Shanghai), Shanghai 200125, China; zhangharewei@163.com (W.Z.); 13601975089@163.com (M.C.); dosfeng@hotmail.com (D.F.)
* Correspondence: yzhao@shou.edu.cn (Y.Z.); yh-zhu@shou.edu.cn (Y.Z.); Tel.: +86-021-61900354 (Y.Z. & Y.Z.)

Abstract: Deltamethrin (DEL) is one of the most commonly used pyrethroid pesticides that can cause serious harms to the ecological environment and human health. Herein, we have developed a paper-based colorimetric sensor impregnated with gold nanoparticles (AuNPs) for on-site determination of DEL pesticide. AuNPs show obvious color change on paper device with the presence of DEL. Measuring the gray intensity of the AuNPs on the reaction zone of the paper sensor allows accurate quantitative analysis. The detection mechanism of DEL on paper sensor was confirmed by UV-Vis spectrophotometry (UV-Vis), Fourier transform infrared spectroscopy (FT-IR), and transmission electron microscope (TEM). Under optimal conditions, the colorimetric sensor exhibited high sensitivity, rapid detection, and low detection limit within the values stipulated by Chinese detection standards (LOD = 0.584 mg/L). Besides, detecting DEL in vegetable and fruit samples also gave satisfying results, which were much consistent with those obtained by spectrophotometry. Overall, this work provided a user-friendly, cost-effective and visualized detection platform, which could be applied to rapidly detect DEL pesticides in the food safety field.

Keywords: colorimetric signal; deltamethrin pesticide; gold nanoparticles; paper sensor; rapid detection

check for updates

Citation: Zhu, J.; Yin, L.; Zhang, W.; Chen, M.; Feng, D.; Zhao, Y.; Zhu, Y. Colorimetric Measurement of Deltamethrin Pesticide Using a Paper Sensor Based on Aggregation of Gold Nanoparticles. *Coatings* **2022**, *12*, 38. https://doi.org/10.3390/coatings12010038

Academic Editor: Arūnas Ramanavičius

Received: 23 November 2021
Accepted: 22 December 2021
Published: 29 December 2021

Publisher's Note: MDPI stays neutral with regard to jurisdictional claims in published maps and institutional affiliations.

Copyright: © 2021 by the authors. Licensee MDPI, Basel, Switzerland. This article is an open access article distributed under the terms and conditions of the Creative Commons Attribution (CC BY) license (https://creativecommons.org/licenses/by/4.0/).

1. Introduction

Deltamethrin (DEL) pesticide, a broad-spectrum systemic pyrethroid, is widely used in agricultural industries due to its excellent insecticidal efficiency [1]. However, the pesticide has long residual lifetime and can easily accumulate in ecosystem, which can cause residues in various food products and environment, affecting the public safety [2–4]. Recently, the toxicology experiments in rats have shown that even a small dose of DEL can result in abnormal pathological reactions in urinary, secretory, immune system [5–7]. Therefore, many countries have enacted the maximum residue level (MRL) of DEL in agricultural products, which has been continually raised in recent years [8].

To date, high-performance liquid chromatography (HPLC) [9], gas spectrometry (GC) [10], and liquid chromatography-mass spectrometry (LC-MS) [11] are preferably applied in the determination of DEL residue. These methods displayed sensitivity and specificity. However, their practical application was hindered due to inevitable limitations including high cost, sophisticated pretreatment, complicated professional operations, and inaccessibility to on-site, real-time monitoring [12,13]. Therefore, it is of great significance to explore a user-friendly, low price, and high efficiency to detect pesticide residues.

Colorimetric sensors provide an effective alternative approach to solve the dilemma for the measurement of pesticide residues [14,15]. Generally, they are easy to fabricate, and the signal can be acquired expediently even by naked eyes. Among various types of colorimetric sensors, the ones based on the nanoparticles (NPs) are becoming more and more attractive for the detection of various hazards because of their interesting advantages,

including high absorption coefficient, high surface area, and localized surface plasmon resonance (LSPR) [16,17]. Adding the target analyte to the NPs solution could induce a shift of LSPR absorption band accompanied by changes in color and particle size [18] Based on the unique physicochemical properties of NPs, a variety of AuNPs colorimetric devices have been established for the highly sensitive detection. Sun et al. reported a colorimetric sensing system based on AuNPs and AChE catalytic reaction with the ultra-high sensitivity to organophosphate pesticide [19]. Brasiunas et al. prepared AuNPs by oxidation–reduction reaction between reducing sugar and $AuCl_4^-$ ions to detect different sugars. [20]. Abnous et al. proposed dsDNA-capped AuNPs for colorimetric detection of malathion in spiked samples [21]. Nevertheless, these colorimetric assays require no less than 5 mL of NPs solution in determination, which is unfavorable, economically speaking [13,22]. Hence, it is highly desirable to develop an alternative approach, which can effectively reduce the reagents consumption in target analyte determination system.

Paper-based microfluidic analytical devices (μPADs) have attracted widespread interest for on-site testing because of their simple, portable, inexpensive, and eco-friendly characteristics [23,24]. The paper-based colorimetric sensors were only according to the measurement of color change because of the chemical reaction between the specific target and corresponding agents (chromogenic reagents/noble metal NPs) coated on paper substrate. This color change, requiring just a small amount of noble metal NPs or other chromogenic reagent, could be not only observed with the naked eye for qualitative analysis, but also be collected by digital camera for quantitative analysis [25,26]. Shrivas et al. developed Cu@Ag core-shell NPs as a sensing probe and combined with paper device for determining residues of phenthoate pesticide in real samples [27]. Wu et al. established a reliable and ultrasensitive paper sensor for organophosphate pesticides analysis, which was mainly related to the enzymatic reaction of AChE and the dissociation characteristic of gold nanoparticles (AuNPs) [28]. Sanyukta et al. summarized recent studies of using noble metal NPs to detect various chemical substances by μPAD [29]. According to these studies, we found that nanoparticles-based paper sensor has great potential in rapid and sensitive pesticides residue detection.

We proposed a simple and economical paper sensor based on aggregation of AuNPs for sensitivity detection of DEL in real samples. AuNPs modified with 2-mercapto-6-nitrobenzothiazole (MNBT) was deposited on paper material as a colorimetric sensor, where the DEL pesticide molecule interacted with the AuNPs. The resulting color intensity was proportional to the sample concentration. The mechanism for detection of DEL was investigated by UV-Vis spectrophotometry (UV-Vis), transmission electron microscopy (TEM), and Fourier transforms infrared spectroscopy (FT-IR). The resulting special driving capacity of the filter paper and the excellent properties of AuNPs led to ultrasensitive detection of the DEL pesticide. Fruit and vegetable samples, tested by the established μPAD method, were also evaluated by spectrum analysis to ensure the accuracy of the experiment results. The study provided a promising approach for facile, sensitive and visual detection of DEL, which has great potential to be generalized to other analyte testing in food analysis.

2. Materials and Methods

2.1. Materials and Chemical Reagents

Whatman filter paper No. 1 (150-mm diameter) was obtained from Whatman International Ltd. (Shanghai, China). Sodium triphosphate pentabasic (NaTPP) (VetecTM reagent grade, CAS No.: 7758-29-4, 98.0%), sodium borohydride ($NaBH_4$) (hydrogen-storage grade, CAS No.: 16940-66-2, 98.0%), chloroauric acid ($HAuCl_4 \cdot xH_2O$) (CAS No.: 27988-77-8, 99.9%+), and deltamethrin (CAS No.: 52918-63-5, 98.0%) were purchased from Sigma-Aldrich (Shanghai, China). Methanol (CH_3OH) (GR, CAS No.: 67-56-1, 99.7%), hydrochloric acid (HCl) (CAS No.: 7647-01-0, 37.0%), sodium hydroxide (NaOH) (AR, CAS No.: 1310-73-2, 96.0%), and ethanol (CH_3CH_2OH) (AR, CAS No.: 64-17-5, 95.0%) were purchased from Sinopharm Chemical Reagent Co., Ltd. (Shanghai, China). 2-Mercapto-

6-nitrobenzothiazole (MNBT) (CAS No.: 4845-58-3, 96.0%) was obtained from Aladdin Industrial Inc. (Shanghai, China). Stock solution of 1 g/L deltamethrin was obtained by methanol and stored for one week. The working solutions were diluted daily by ultrapure water to various concentrations. All solutions were prepared with ultrapure water provided by Millipore system (Millipore Corp., Bedford, MA, USA) with a resistivity of 18.2 MΩ.

2.2. Instruments and Software

UV-Vis spectrophotometer (JASCO, Model V-570, Tokyo, Japan) was utilized to collect the UV–Vis absorption spectra. The morphology and particle size of the synthesized nanoparticles were measured by transmission electron microscope (TEM, JEOL-2100F, Tokyo, Japan).

Auto CAD software (Version 2016) was performed to design the patterns of μPAD. The designed pattern was cut by a FST Laser cutting 1530. The color photos of μPAD were taken by a Canon OD60 camera with high resolution. The images were converted to RGB value by Image J software and the RGB value of sensing area was converted into grayscale for quantitative analysis.

2.3. Nanoparticles Synthesis

The gold nanoparticles (AuNPs) used in this work were prepared based on the previous study with some modifications [30]. First, 200.0 mL of $HAuCl_4 \cdot 3H_2O$ solution (0.5 mmol/L) and 5.0 mL of $NaBH_4$ (0.2 mol/L) were mixed together for 30 min, which finally turned into shiny red (Scheme 1a). For preparation of functionalized AuNPs, 30.0 μL MNBT (1.2 mmol/L) was added into 40.0 mL AuNPs, and the mixed solution was stirred at 150 rpm for 120 min. The MNBT was adsorbed onto the surface of the AuNPs via Au-S atom to form core-shell structure. The prepared MNBT-AuNPs were stored at 4 °C for later use.

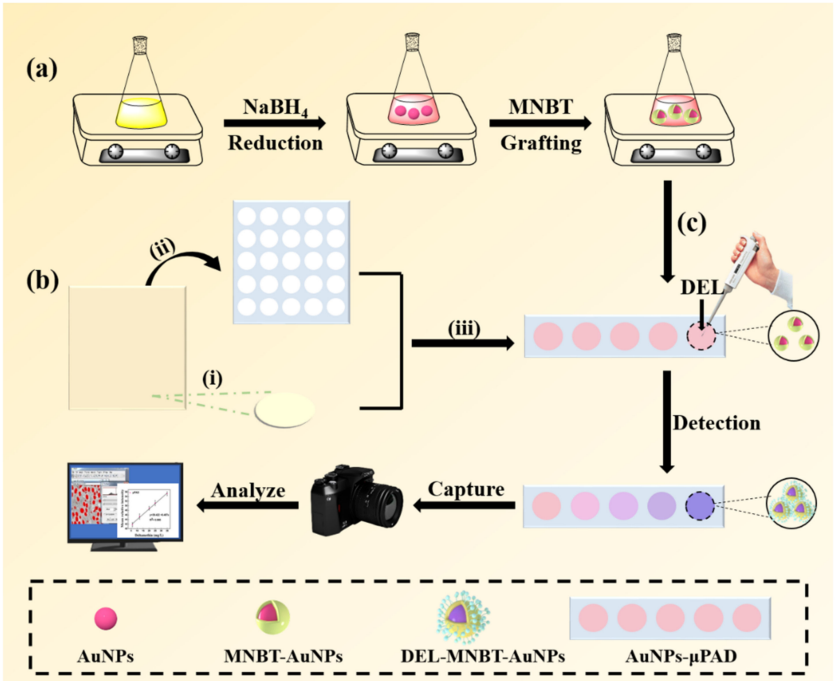

Scheme 1. Schematic diagram of (**a**) Synthesis of MNBT-AuNPs; (**b**) the fabrication process of the μPAD: (i) cutting the reaction zone, (ii) fabricating the hydrophobic paper channels, and (iii) placing the reaction zone onto the hydrophobic paper channels to prepare the paper analytical device. (**c**) The steps of DEL assay using the colorimetric μPAD.

2.4. Fabrication of Microfluidic Paper Device (μPAD)

The process of fabrication is depicted in Scheme 1b, which is mainly subdivided into three measures: First, the reaction zone pattern of filter paper was designed by Auto CAD 2016 software and cut into suitable size by laser cutting. After cutting, the remaining paper was hydrophobicized with the TEMS solution for 1 min and dried in oven for 1 h. Finally, the cut circular detection area was installed on the hydrophobic channels to prepare the paper analytical device.

2.5. Sensing Procedure and Data Processing

Scheme 1c shows how the μPAD is used for detection of DEL. First, the μPAD was pretreated with 10.0 μL AuNPs. Then, 2.0 μL DEL pesticide with buffer solution was added to the pretreatment zone to generate a specific color signal. After the signal was stable (within 20 min), the sensor images were captured with a digital camera. For each sensing area, the color of images was calculated with Image J.

The Image J translated the intensity of captured images into three numerical averages corresponding to the color elements of red, green, and blue. The differences in color intensity before and after reaction were calculated by the following formula:

$$\Delta R = \overline{R}_{after} - \overline{R}_{before}$$

$$\Delta G = \overline{G}_{after} - \overline{G}_{before}$$

$$\Delta B = \overline{B}_{after} - \overline{B}_{before}$$

According to this formula, the difference values of three elements were represented by ΔR, ΔG, and ΔB, respectively. Next, the difference values between the reaction point and the blank point were reconverted to gray intensity by the following equations:

$$\Delta Gray = 0.30\Delta R + 0.59\Delta G + 0.11\Delta B$$

Furthermore, more accurate detection could be achieved by matching the gray value and absorbance signal. The experiment for detection of DEL with UV-Vis spectrophotometry (UV-3900H), in solution state, was proceeded. The absorbance was obtained at the maximum absorption peak (516 nm) to calculate the absorbance change rate using the formula ($A_0$516–A516)/A516. Herein, $A_0$516 represented the absorbance of bare MNBT-AuNPs; A516 expressed the absorbance in the presence of DEL and ($A_0$516 − A516)/A516 represented the absorption change rate of AuNPs.

All experiments were repeated independently three times.

2.6. Real Samples Pretreatment and Measurements

Five kinds of fresh fruits and vegetables were selected as verification samples to detect the level of DEL pesticide residues to investigate the performance of the established sensor in practical application. These fruits and vegetables were procured from a supermarket located in Shanghai. The detailed sample pretreatment process was performed according to GB 29705-2013 and GB/T 2763-2019 [31,32]. Briefly, each sample (20.0 g) was homogenized followed by extracting with 40 mL of acetonitrile. After centrifugation, 4 mL of the supernatant was taken and further passed through a 0.22 μm microporous porosity filter to minimize the interference of impurities. Finally, the extracted filtrate was diluted five times with the buffer solution. The processing of samples was carried out freshly just before test. Each vegetable sample was spiked with two concentrations of DEL, and tested at least three times with the μPAD.

To prove the reliability of the μPAD, contrast experiment for detection of DEL using UV-Vis spectrophotometry was also performed following the same pretreatment steps for μPAD method.

2.7. Statistical Analysis

Statistical significance was examined through Student's *t* test or one-way analysis of variance (ANOVA) at $p < 0.05$ using the SigmaStat software (Version 3.5).

3. Results

3.1. Mechanism of AuNPs Detecting DEL

Figure 1 shows the FT-IR spectra of AuNPs, MNBT, MNBT-AuNPs, DEL, and DEL-MNBT-AuNPs at the wavenumber of 400 to 4000 cm^{-1}. Compared with the AuNPs, the FT-IR spectrum of MNBT- AuNPs showed characteristic peaks of MNBT (stretching vibration of –CH of benzene ring at 2931 cm^{-1}, skeleton vibration of the benzene ring at 1378 cm^{-1}, stretching vibration of N=O at 1450 cm^{-1} and strong Au-S bond at 810 cm^{-1}) (Figure 1) [33]. Besides, the FT-IR spectrum of DEL-MNBT-AuNPs (Figure 1) not only exhibited characteristic peaks consistent with MNBT-AuNPs, but also presented new absorption peaks (symmetric stretching of C–O–C at 1133 cm^{-1} and stretching vibration of C-Br at 978 cm^{-1}).

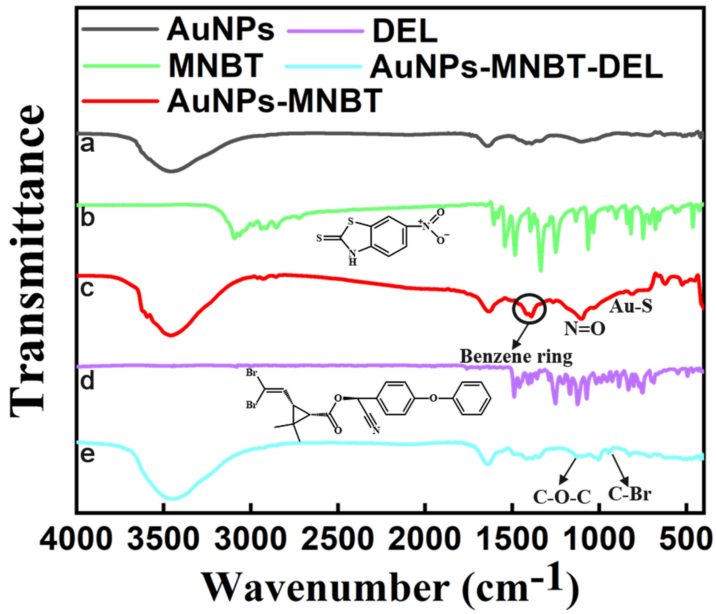

Figure 1. The FT-IR spectra of a—AuNPs, b—MNBT, c—MNBT-AuNPs, d—DEL, and **e**—DEL-MNBT-AuNPs.

Figure 2a shows the absorption spectra change for the AuNPs using the UV-Vis spectrophotometer (JASCO, Model V-570) at the range of 350–600 nm. As shown in Figure 2a, AuNPs had a surface plasma resonance (SPR) absorption peak at 516 nm. After adding DEL, the absorption peak of AuNPs shifted significantly to 524 nm accompanied by a color change from red to purple, and the absorbance also decreased obviously. Meanwhile, the morphology of the AuNPs-MNBT was observed by transmission electron microscope type JEOL-2100F (Japan). Figure 2b,c showed TEM morphologies of AuNPs-MNBT under different magnification, which presented a well-dispersed spherical structure. The diameter was measured to be ~5 nm which was estimated by the Image J software (the inset of Figure 2b). After the DEL addition, the morphology of MNBT-AuNPs aggregated into large particles (Figure 2d).

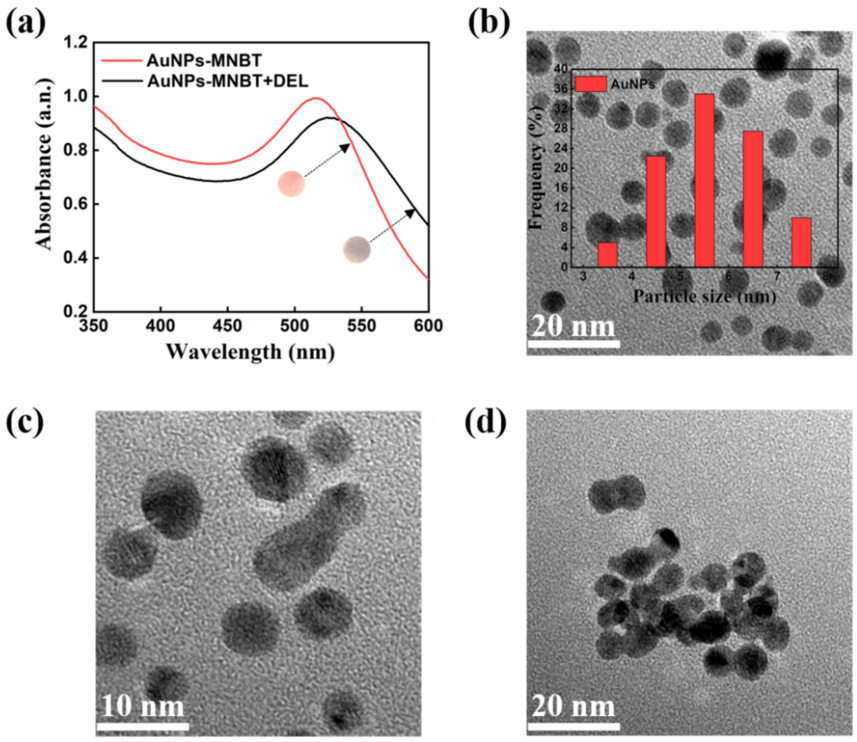

Figure 2. (**a**) UV–visible absorption spectra of MNBT-AuNPs and MNBT-AuNPs-DEL. (**b**,**c**) TEM images (insert is the particle size distribution) of MNBT-AuNPs and (**d**) MNBT-AuNPs-DEL.

3.2. Effect of AuNPs Synthesis Condition

The principle of DEL analysis is displayed in Figure 3a. The MNBT as ligand was used for the synthesis of AuNPs-MNBT, which formed a strong Au-S bond to AuNPs through a self-assembly method. After addition of DEL, the benzene ring on MNBT and another one on DEL form a core-shell structure by a π-π stacking effect [30]. Considering that the AuNPs can be significantly influenced by the synthesis condition, we optimized the concentration of reducing agent and MNBT in the route of synthesizing gold nanoparticles to provide stable AuNPs that offer rapid response and repeatable detection performance in subsequent experiments. The $NaBH_4$ solution with different concentrations was added to 10.0 mL of $HAuCl_4$ solution to form AuNPs. As shown in Figure 3b, the color of AuNPs changed from yellow to red and finally to gray purple as the $NaBH_4$ concentration increased [34]. The AuNPs absorbance value was significantly higher in the condition of 0.2 mol/L $NaBH_4$ compared with other concentration. Therefore, the 0.2 mol/L $NaBH_4$ was selected to synthesize stable AuNPs for further experiments.

The concentration of MNBT is crucial to initiate the aggregation reaction. As shown in Figure 3c, it was found that increasing MNBT concentration from 0.3 to 1.2 mmol/L led to a remarkable increase of mean relative intensity. But further increase from 1.2 to 1.5 mmol/L resulted in a clear decline. Therefore, the AuNPs system was most beneficial for the detection of DEL pesticides in 1.2 mmol/L.

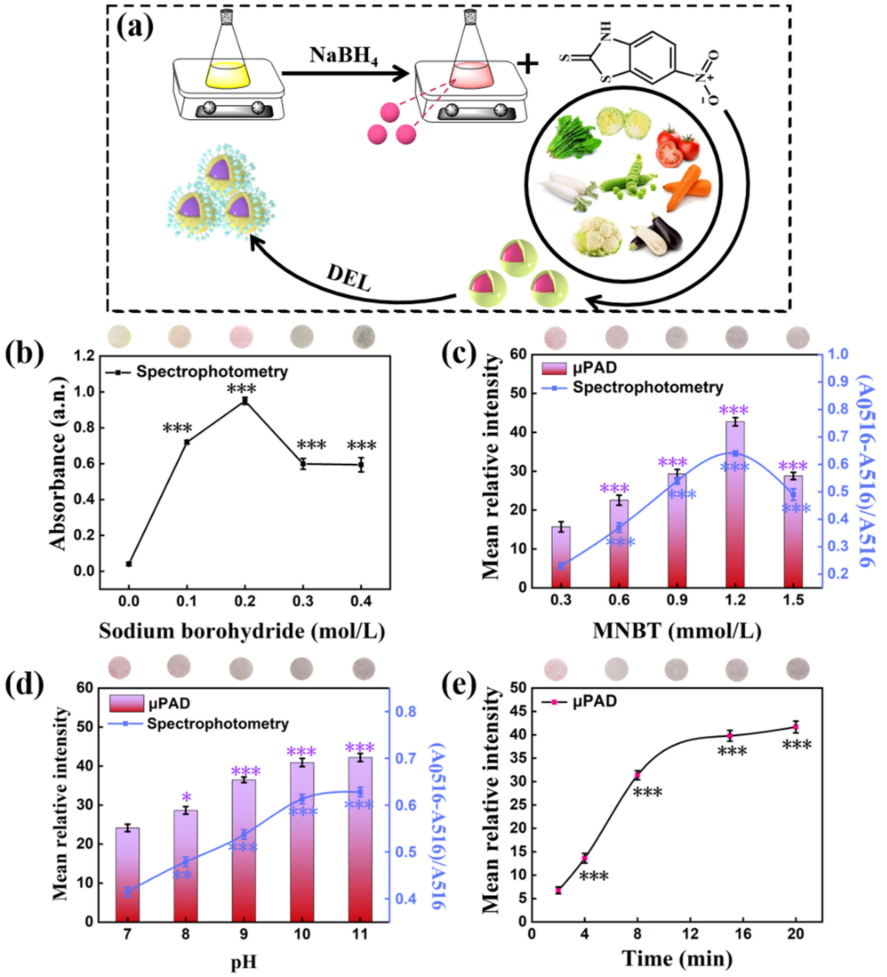

Figure 3. The determination for DEL by paper sensor and spectrophotometric method. (**a**) AuNPs detection principle for DEL. The effect of (**b**) concentration of $NaBH_4$ (*** $p < 0.001$ compared to Sodium borohydride 0.0 mol/L condition), (**c**) the concentration of MNBT (*** $p < 0.001$ compared to MNBT 0.3 mmol/L condition), (**d**) pH of system buffer and (*** $p < 0.001$, compared to pH 7 condition) (**e**) the reaction time (*** $p < 0.001$ compared to Time 2 min condition).

3.3. Optimization of Reaction Conditions

Meanwhile, the pH of the AuNPs system was optimized. Under different pH condition, the mean relative intensity of μPAD after the addition of DEL is shown in Figure 3d. When the applied value of pH increased from 7.0 to 11.0, the mean relative intensity gradually increased to reach a maximum value at 11.0. Based on this observation, the final pH was set as 11.0 in following experiments.

Figure 3e illustrated the dependence of sensor color intensity on reaction time changing from 0 to 20 min. The mean relative intensity is positively proportional to the reaction time and then displays no clear increase beyond 20 min of reaction. Hence, the reaction time was chosen as 20 min for subsequent color analysis.

3.4. Sensitive Detection of DEL

Under the above optimal conditions, experiments were performed by adding target DEL with different concentrations onto the μPAD to observe whether the change of mean relative intensity could be used for DEL quantification. In Figure 4a, the color intensity of MNBT-AuNPs coated on μPAD increased with a rise in the concentration of DEL. A good linear relationship ($R^2 = 0.995$) between the mean relative intensity of μPAD and the concentration of DEL was obtained in the range from 6.0 to 35.0 mg/L (Figure 4b). The estimated linear correlation equation was: y = 39.422 + 0.407x (y, mean relative intensity;

x, deltamethrin concent L). Meanwhile, contrast experiments were accomplished by spectrophotometry. The results showed that the absorption level decreased gradually with increasing concentrations of DEL (Figure 4c). Moreover, the results clearly indicated that a good linear equation of DEL (y = 0.047 + 0.075x, R^2 = 0.993, LOD = 0.173 mg/L) was obtained (Figure 4d). In order to evaluate the selectivity of the paper sensing platform to DEL pesticides, the color change of AuNPs to varieties of pesticides was investigated at the same detection condition (Figure S2). By comparison, the color has no obvious change in the presence of other pesticides (dimethoate, dichlorvos, and fenpropathrin) at 20 mg/L.

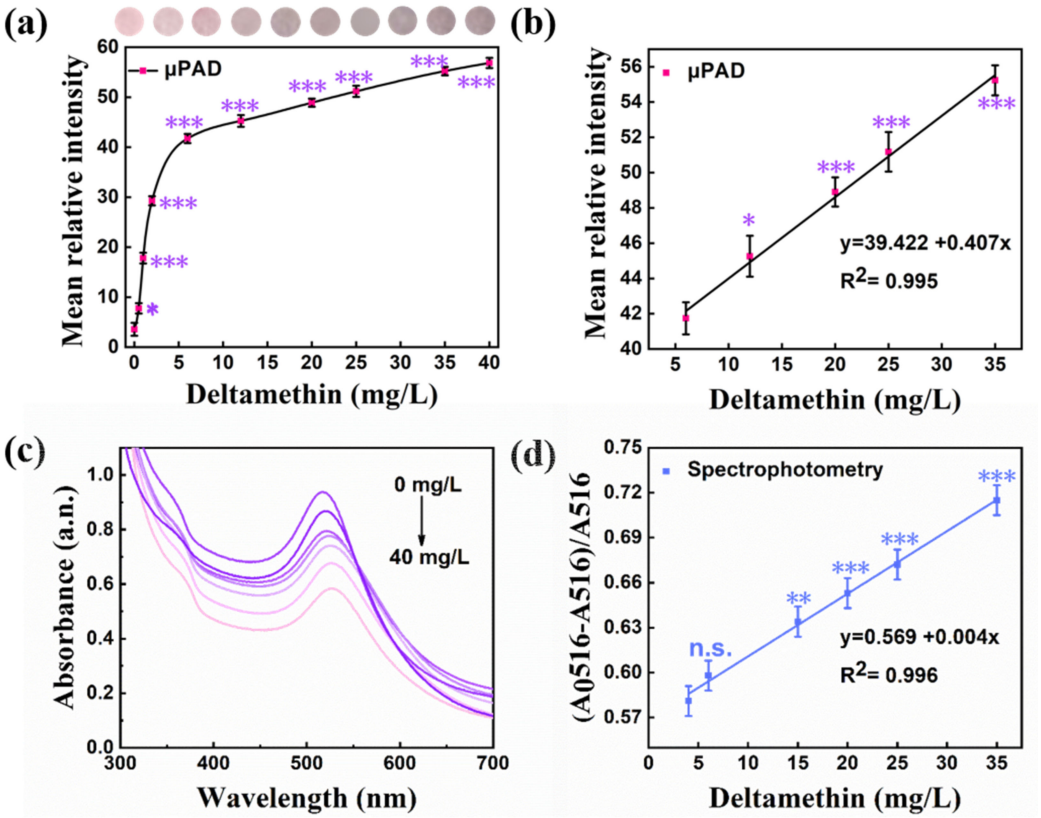

Figure 4. (**a**) The dependence of mean relative intensity on the concentration of DEL (* $p < 0.5$ and *** $p < 0.001$, compared to Deltamethin 0.1 mg/L condition). (**b**) The linear relationship between DEL concentration and gray intensity of μPAD (* $p < 0.5$ and *** $p < 0.001$ compared to Deltamethin 6 mg/L condition). (**c**) The dependence of absorption spectrum on the concentration of DEL. (**d**) The linear relationship between DEL concentration with absorption ratio of spectrophotometry (n.s., not significant, ** $p < 0.01$ and *** $p < 0.001$ compared to Deltamethin 4 mg/L condition).

3.5. Application of the μPAD to Detect DEL in Fruit and Vegetable

The ability of the sensor for detecting DEL in actual samples, including apple, mandarin orange, spinach, tomato, and cucumber contaminated by DEL was investigated. The content of DEL is listed in Table 1. The amount of DEL in different real samples was estimated by spectrophotometry and colorimetric method. As reported in Table 1, the relative recovery rate of the pesticide detected by the μPAD was 92.8–104.3%, and the relative standard deviations were 2.2–6.5%.

Table 1. Comparison of DEL detection results in various fruits and vegetables using the μPAD versus the spectrophotometry (ND, undetectable and *** $p < 0.001$ compared to untreated samples condition).

Sample	Found	Added (mg/L)	DEL Concentration (mg/L)		Statistical Significance		RSD (%) (n = 3)	
			μPAD	Spectrophotometry	μPAD	Spectrophotometry	μPAD	Spectrophotometry
Apple	ND	10	10.29	9.98	***	***	4.9	5.5
	ND	20	19.83	20.31	***	***	2.2	2.7
mandarin	ND	10	9.89	10.38	***	***	3.8	4.1
orange	ND	20	19.21	21.11	***	***	3.7	3.2
spinach	ND	10	10.04	9.53	***	***	4.2	3.5
	ND	20	20.17	19.57	***	***	2.8	3.7
tomato	ND	10	9.28	9.32	***	***	5.3	4.7
	ND	20	20.85	18.88	***	***	3	4.3
cucumber	ND	10	9.58	10.62	***	***	5.2	4.8
	ND	20	20.02	20.24	***	***	6.5	6.2

4. Discussion

4.1. Mechanism of AuNPs Detecting DEL

The FT-IR spectra prove the functionalization of the synthesized AuNPs (Figure 1). After MNBT grafting, the C–H peak appeared because the number of benzene ring increased during the grafting process. The new peak originated from the N=O stretching vibration of MNBT appeared in AuNPs-MNBT spectra as well. Besides, the peak around 810 cm^{-1} illustrated the Au-S stretching vibration. These above results imply that MNBT is successfully anchored onto AuNPs (Figure 1). Compared to the modified AuNPs in Figure 1, the new peaks were found when the DEL was added (Figure 1). The characteristic peak forms around 1133 cm^{-1} which is regarded as the symmetric stretching of C–O–C from the DEL. A new peak that originated from the C-Br stretching vibration of DEL appears at 978 cm^{-1} as well. Therefore, the results confirm that the DEL was successfully reacted with MNBT-AuNPs.

According to the UV-vis analysis and TEM characterization (Figure 2), the addition of DEL had obvious effect on the AuNPs colorimetric probe. The significant shift of the obtained absorption spectrum indicated the interaction between DEL and AuNPs. Moreover, the DEL-treated material had a higher aggregation structure than the untreated material. The π-π stacking interaction occurred in the combination of DEL and MNBT-AuNPs. Figure S1 explained the mechanism by which DEL induces MNBT-AuNPs aggregation.

4.2. Effect of Synthesis Condition

The strong reducing property of $NaBH_4$ makes it a suitable reductant for synthesis of the AuNPs. Zhang et al. reported the impact of $NaBH_4$ concentration on the performance of AuNPs [34]. This research results pointed that excessive $NaBH_4$ would affect the stability of AuNPs due to the increased number of electrons, which was consistent with our phenomenon in Figure 3b. Furthermore, the AuNPs with different concentrations of MNBT directly impacted the detection effect of DEL. Figure 3c represents that as the concentration of MNBT was 1.2 mmol/L, the color change was most obvious, which was conductive to visual observation. The MNBT was not suitable for DEL detection under the low concentration. In high MNBT content, the reaction between the free MNBT to free in the solution and DEL intensified the aggregation of AuNPs.

4.3. Optimization of Reaction Conditions

Recently, Li et al. and Chen et al. considered the optimization of pH of buffer solutions and incubation time as the main experiments for the development of a successful colorimetric method [35,36]. The results of Figure 3d revealed that the AuNPs-MNBT system with the largest change in pH = 11.0 buffer. The powerful hydrolysis of DEL occurred in alkaline media, which reduced the steric hindrance of AuNPs and was more favorable for the reaction [37]. The effect of reaction time was also shown in Figure 3e. The color changed markedly with the reaction time and tend to stabilize when the time reached

20 min. The result further illustrates the paper sensor needs less reaction time of the assay, which can achieve the determination of DEL conveniently and fast.

4.4. Sensitive Detection of DEL

Compared with traditional single signal sensor for pesticide, the proposed μPAD was further combined with spectrophotometry, which not only avoided the false positive signal caused by detection condition and operation situation, but also expanded the detection ranges and improved the accuracy. As shown in Figure 4, a good linear relationship and R-squared were required. The LOD was lower than the China defined MRL (2 mg/L) of DEL [31,32]. Moreover, satisfying results were acquired from spectrophotometry in the DEL detecting, which were much agreed well with those obtained by μPAD. In addition, selectivity is an important indicator in the performance evaluation. It can be obviously found that no significant change in the color intensity resulted from all the pesticides except DEL, which is due to the different structure of pesticides (Figure S2). This indicates that the interference from other pesticides is negligible in the determination of DEL by the μPAD. As a result, the μPAD could detect DEL with high sensitivity and high specificity.

4.5. Application of the μPAD to Detect DEL in Fruit and Vegetable

To implement μPAD with the screening of DEL in food, fruits and vegetables were used as a representative food samples, which were carefully pre-processed, including organic solvent extraction, membrane filtration, and sample filtrate dilution. As illustrated in Table 1, the paper sensor was successfully employed in the detection of DEL in the fruits and vegetables using MNBT-AuNPs. Therefore, the developed μPAD possesses promising potential for the determination of DEL in the real samples.

5. Conclusions

In summary, a device for rapid detection of DEL in real samples was proposed by utilizing a simple colorimetric method. The presence of DEL was demonstrated by a visualized colorimetric assay through the formation of functionalized AuNPs aggregate. Buffers and chromogenic reagents were first pre-stored on each detection area in a dry form. The mean relative intensity of the photos was obtained by image J when the user added only 10 μL sample solution in the test area. Due to its great advantages like portability, low price, ready availability, and facile on-site detection without particular request of technical personnel, μPAD could be applied in farms, supermarkets, and even domestic areas to ensure food safety. We also hope to extend the potential applications toward point-of-care fields, e.g., biological contaminants or nutrient detection. Hence, the portable device offers a valuable insight for field analysis in the future.

Supplementary Materials: The following supporting information can be downloaded at: https://www.mdpi.com/article/10.3390/coatings12010038/s1, Figure S1: Schematic illustration of possible π-π stacking mechanism for aggregation of MNBT-AuNPs in the presence of DEL; Figure S2. Selectivity of the μPAD to different pesticide molecules, including dimethoate, di-chlorvos, fenpropathrin, and deltamethrin. (n.s., not significant and *** $p < 0.001$ compared to Blank condition).

Author Contributions: Conceptualization, Y.Z. (Yongheng Zhu); methodology, J.Z. and L.Y.; software, J.Z.; validation, Y.Z. (Yongheng Zhu) and Y.Z. (Yong Zhao); formal analysis, J.Z.; investigation, J.Z.; resources, Y.Z. (Yongheng Zhu) and Y.Z. (Yong Zhao); data curation, J.Z.; writing—original draft preparation, J.Z., L.Y. and W.Z.; writing—review and editing, J.Z., M.C. and D.F.; visualization, J.Z. and W.Z.; supervision, Y.Z. (Yongheng Zhu); project administration, Y.Z. (Yongheng Zhu); funding acquisition, Y.Z. (Yongheng Zhu). All authors have read and agreed to the published version of the manuscript.

Funding: This research was funded by the Key Project of Shanghai Agriculture Prosperity through Science and Technology (2019-02-08-00-15-F01147). The authors sincerely thank all the panelists for experimental support.

Institutional Review Board Statement: Not applicable.

Informed Consent Statement: Not applicable.

Data Availability Statement: The data presented in this study are available on request from the corresponding author.

Conflicts of Interest: The authors declare no conflict of interest.

References

1. Guo, T.; Wang, C.; Zhou, H.; Zhang, Y.; Ma, L. A multifunctional near-infrared fluorescent sensing material based on core-shell upconversion nanoparticles@magnetic nanoparticles and molecularly imprinted polymers for detection of deltamethrin. *Microchim Acta.* **2021**, *188*, 165. [CrossRef]
2. Bhamore, J.R.; Jha, S.; Singhal, R.K.; Murthy, Z.V.P.; Kailasa, S.K. Amylase protected gold nanoclusters as chemo- and bio- sensor for nanomolar detection of deltamethrin and glutathione. *Sens. Actuators B Chem.* **2019**, *281*, 812–820. [CrossRef]
3. Liu, X.; Li, L.; Liu, Y.Q.; Shi, X.B.; Li, W.J.; Yang, Y.; Mao, L.G. Ultrasensitive detection of deltamethrin by immune magnetic nanoparticles separation coupled with surface plasmon resonance sensor. *Biosens. Bioelectron.* **2014**, *59*, 328–334. [CrossRef]
4. Bissacot, D.Z.; Vassilieff, I. Pyrethroid residues in milk and blood of dairy cows following single topical applications. *Vet. Hum. Toxicol.* **1997**, *39*, 6–8.
5. Vinggaard, A.M.; Christiansen, S.; Laier, P.; Poulsen, M.E.; Breinholt, V.; Jarfelt, K.; Jacobsen, H.; Dalgaard, M.; Nellemann, C.; Hass, U. Perinatal exposure to the fungicide prochloraz feminizes the male rat offspring. *Toxicol. Sci.* **2005**, *85*, 886–897. [CrossRef]
6. Poulsen, C.R.; Bokvist, K.; Olsen, H.L.; Hoy, M.; Capito, K.; Gilon, P.; Gromada, J. Multiple sites of purinergic control of insulin secretion in mouse pancreatic beta-cells. *Diabetes* **1999**, *48*, 2171–2181. [CrossRef] [PubMed]
7. El-Sayed, Y.S.; Saad, T.T.; El-Bahr, S.M. Acute intoxication of deltamethrin in monosex Nile tilapia, Oreochromis niloticus with special reference to the clinical, biochemical and haematological effect. *Environ. Toxicol. Pharmacol.* **2007**, *24*, 212–217. [CrossRef]
8. Brancato, A.; Brocca, D.; De Lentdecker, C.; Erdos, Z.; Ferreira, L.; Greco, L.; Jarrah, S.; Kardassi, D.; Leuschner, R.; Lythgo, C.; et al. Modification of the existing maximum residue level for deltamethrin in kale. *EFSA J.* **2018**, *16*, 5153–5179.
9. Boonchiangma, S.; Ngeontae, W.; Srijaranai, S. Determination of six pyrethroid insecticides in fruit juice samples using dispersive liquid-liquid microextraction combined with high performance liquid chromatography. *Talanta* **2012**, *88*, 209–215. [CrossRef] [PubMed]
10. Zhu, P.; Fan, S.; Zou, J.H.; Miao, H.; Li, J.G.; Zhang, G.W.; Wu, Y.N. Application of Gas Chromatography-mass Spectrometry in Analyzing Pharmacokinetics and Distribution of Deltamethrin in Miniature Pig Tissues. *Biomed. Environ. Sci.* **2014**, *27*, 426–435.
11. Kobayashi, H. Development of Residue Analysis for Pesticides by LC/MS and LC/MS/MS Methods. *Bunseki Kagaku* **2009**, *58*, 985–997. [CrossRef]
12. Diaz-Amaya, S.; Zhao, M.; Allebach, J.P.; Chiu, G.T.; Stanciu, L.A. Ionic Strength Influences on Biofunctional Au-Decorated Microparticles for Enhanced Performance in Multiplexed Colorimetric Sensors. *ACS Appl. Mater. Inter.* **2020**, *12*, 32397–32409. [CrossRef]
13. Monisha; Shrivas, K.; Kant, T.; Patel, S.; Devi, R.; Dahariya, N.S.; Pervez, S.; Deb, M.K.; Rai, M.K.; Rai, J. Inkjet-printed paper-based colorimetric sensor coupled with smartphone for determination of mercury (Hg^{2+}). *J. Hazard. Mater.* **2021**, *414*, 125440. [CrossRef]
14. Lee, M.G.; Patil, V.; Na, Y.-C.; Lee, D.S.; Lim, S.H.; Yi, G.-R. Highly stable, rapid colorimetric detection of carbaryl pesticides by azo coupling reaction with chemical pre-treatment. *Sens. Actuators B Chem.* **2018**, *261*, 489–496. [CrossRef]
15. Sun, Z.W.; Tian, L.Y.; Guo, M.; Xu, X.T.; Li, Q.; Weng, H.B. A double-film screening card for rapid detection of organophosphate and carbamate pesticide residues by one step in vegetables and fruits. *Food Control.* **2017**, *81*, 23–29. [CrossRef]
16. Dong, L.; Hou, C.; Yang, M.; Fa, H.; Wu, H.; Shen, C.; Huo, D. Highly sensitive colorimetric and fluorescent sensor for cyanazine based on the inner filter effect of gold nanoparticles. *J. Nanopart. Res.* **2016**, *18*, 164. [CrossRef]
17. Shariati, S.; Khayatian, G. Microfluidic paper-based analytical device using gold nanoparticles modified with N,N′-bis(2-hydroxyethyl)dithiooxamide for detection of Hg^{2+} in air, fish and water samples. *New J. Chem.* **2020**, *44*, 18662–18667. [CrossRef]
18. Elahi, N.; Kamali, M.; Baghersad, M.H. Recent biomedical applications of gold nanoparticles: A review. *Talanta* **2018**, *184*, 537–556. [CrossRef] [PubMed]
19. Sun, J.; Guo, L.; Bao, Y.; Xie, J. A simple, label-free AuNPs-based colorimetric ultrasensitive detection of nerve agents and highly toxic organophosphate pesticide. *Biosens. Bioelectron.* **2011**, *28*, 152–157. [CrossRef] [PubMed]
20. Brasiunas, B.; Popov, A.; Ramanavicius, A.; Ramanaviciene, A. Gold nanoparticle based colorimetric sensing strategy for the determination of reducing sugars. *Food Chem.* **2021**, *351*, 129238. [CrossRef]
21. Abnous, K.; Danesh, N.M.; Ramezani, M.; Alibolandi, M.; Emrani, A.S.; Lavaee, P.; Taghdisi, S.M. A colorimetric gold nanoparticle aggregation assay for malathion based on target-induced hairpin structure assembly of complementary strands of aptamer. *Mikrochim. Acta.* **2018**, *185*, 216. [CrossRef]
22. Chang, C.C.; Chen, C.P.; Wu, T.H.; Yang, C.H.; Lin, C.W.; Chen, C.Y. Gold Nanoparticle-Based Colorimetric Strategies for Chemical and Biological Sensing Applications. *Nanomaterials* **2019**, *9*, 861. [CrossRef]
23. Tai, H.; Duan, Z.; Wang, Y.; Wang, S.; Jiang, Y. Paper-Based Sensors for Gas, Humidity, and Strain Detections: A Review. *Acs Appl. Mater. Inter.* **2020**, *12*, 31037–31053. [CrossRef] [PubMed]
24. Zhang, D.; Li, C.; Ji, D.; Wang, Y. Paper-Based Microfluidic Sensors for Onsite Environmental Detection: A Critical Review. *Crit. Rev. Anal. Chem.* **2021**, *3*, 1–40. [CrossRef] [PubMed]

25. Shrivas, K.; Kant, T.; Karbhal, I.; Kurrey, R.; Sahu, B.; Sinha, D.; Patra, G.K.; Deb, M.K.; Pervez, S. Smartphone coupled with paper-based chemical sensor for on-site determination of iron(III) in environmental and biological samples. *Anal. Bioanal. Chem.* **2020**, *412*, 1573–1583. [CrossRef] [PubMed]
26. Shrivas, K.; Nirmalkar, N.; Ghosale, A.; Thakur, S.S. Application of silver nanoparticles for a highly selective colorimetric assay of endrin in water and food samples based on stereoselective endo-recognition. *RSC Adv.* **2016**, *6*, 29855–29862. [CrossRef]
27. Shrivas, K.; Monisha; Patel, S.; Thakur, S.S.; Shankar, R. Food safety monitoring of the pesticide phenthoate using a smartphone-assisted paper-based sensor with bimetallic Cu@Ag core-shell nanoparticles. *Lab Chip* **2020**, *20*, 3996–4006. [CrossRef]
28. Wu, S.; Li, D.; Wang, J.; Zhao, Y.; Dong, S.; Wang, X. Gold nanoparticles dissolution based colorimetric method for highly sensitive detection of organophosphate pesticides. *Sens. Actuators B Chem.* **2017**, *238*, 427–433. [CrossRef]
29. Patel, S.; Jamunkar, R.; Sinha, D.; Monisha; Patle, T.K.; Kant, T.; Dewangan, K.; Shrivas, K. Recent development in nanomaterials fabricated paper-based colorimetric and fluorescent sensors: A review. *Trends Environ. Anal.* **2021**, *31*, e00136. [CrossRef]
30. Wang, Z.; Huang, Y.; Wang, D.; Sun, L.; Dong, C.; Fang, L.; Zhang, Y.; Wu, A. A rapid colorimetric method for the detection of deltamethrin based on gold nanoparticles modified with 2-mercapto-6-nitrobenzothiazole. *Anal. Methods* **2018**, *10*, 1774–1780. [CrossRef]
31. *GB29705-2013*; Food Safety National Standard—Determination of Organophosphorus Multi Pesticides Residue in Foods Gas Chromatography-Mass Spectrometry. The Standardization Administration of the People's Republic of China: Beijing, China, 2016.
32. *GB5009.110-2003*; Determination of Cypermethrin, Fenvalerate and Deltamethrin Residues in Vegetable Foods. The Standardization Administration of the People's Republic of China: Beijing, China, 2003.
33. Dasary, S.S.R.; Zones, Y.K.; Barnes, S.L.; Ray, P.C.; Singh, A.K. Alizarin Dye based ultrasensitive plasmonic SERS probe for trace level Cadmium detection in drinking water. *Sens. Actuators. B Chem.* **2016**, *224*, 65–72. [CrossRef] [PubMed]
34. Zhang, Z.; Wu, Y. Investigation of the $NaBH_4$-induced aggregation of Au nanoparticles. *Langmiur* **2010**, *26*, 9214–9223. [CrossRef] [PubMed]
35. Li, J.J.; Ni, T.J.; Liu, H.Q.; Wu, L.; Pan, Y.J.; Zhao, Y.; Zhu, Y.H. Functional poly(carboxybetaine methacrylate) coated paper sensor for high efficient and multiple detection of nutrients in fruit. *Chin. Chem. Lett.* **2020**, *31*, 1099–1103. [CrossRef]
36. Chen, H.Y.; Hu, O.; Fan, Y.; Lu, X.; Zhang, L.; Lan, W.; Hu, Y.; Xie, X.R.; Ma, L.X.; She, Y.B.; et al. Fluorescence paper-based sensor for visual detection of carbamate pesticides in food based on CdTe quantum dot and nano ZnTPyP. *Food Chem.* **2020**, *327*, 127075. [CrossRef] [PubMed]
37. Gupta, S.; Handa, S.K.; Sharma, K.K. A new spray reagent for the detection of synthetic pyrethroids containing a nitrile group on thin-layer plates. *Talanta* **1998**, *45*, 1111–1114. [CrossRef]